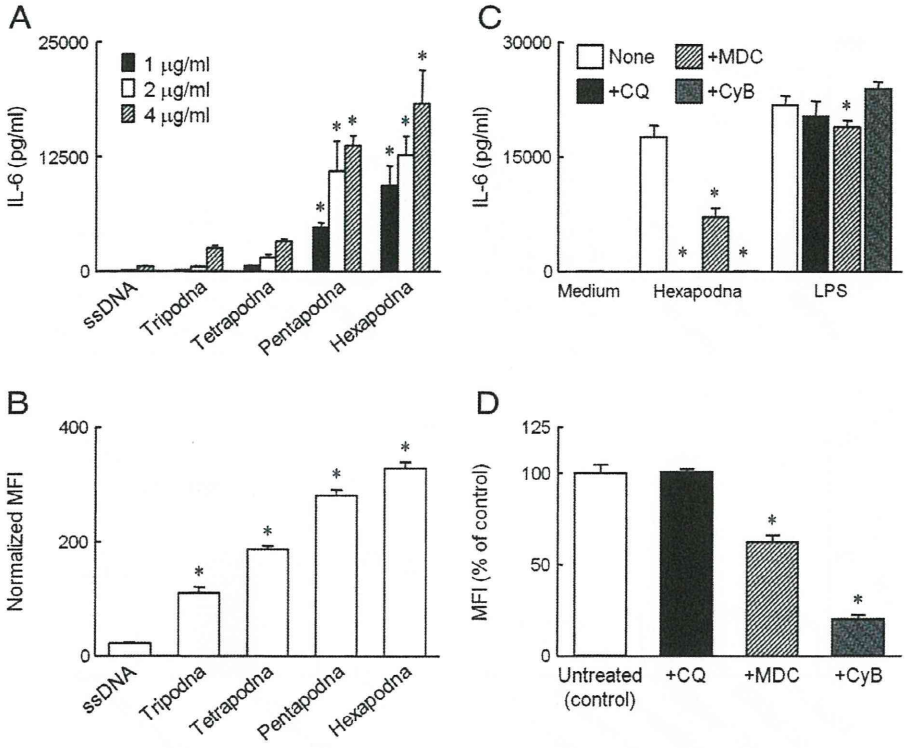

Figure 2. IL-6 release and uptake of ssDNA or polypodna after addition to mouse dendritic DC2.4 cells. **(A)** DC2.4 cells were treated with ssDNA or polypodna at a final concentration of 1, 2 or 4 μg/mL and incubated at 37 °C for 24 h. The concentrations of IL-6 in culture media were measured by ELISA. Results are expressed as mean ± SD of four wells. Data are representative of three independent experiments. *$P < 0.05$ compared with the ssDNA-treated group. **(B)** DC2.4 cells were treated with Alexa Fluor 488-labelled ssDNA or polypodna at a final concentration of 2 μg/mL and incubated at 37 °C for 8 h. The amounts of DNA associated with the cells were measured by flow cytometry, and the normalized MFI was calculated to compare the cellular uptake of DNA samples. Results are expressed as mean ± SD of six wells. Data are representative of three independent experiments. *$P < 0.05$ compared with the ssDNA-treated group. **(C)** DC2.4 cells were incubated with none, 6.25 μM chloroquine (CQ), 25 μM monodansylcadaverine (MDC), or 5 μM cytochalasin B (CyB) for 30 min, then treated with hexapodna (2 μg/mL) or LPS (25 ng/mL) and incubated at 37 °C for 24 h. The concentrations of IL-6 in culture media were measured by ELISA. Results are expressed as mean ± SD of four wells. Data are representative of two independent experiments. *$P < 0.05$ compared with the untreated (control) groups. **(D)** DC2.4 cells were incubated with none, 6.25 μM chloroquine (CQ), 25 μM monodansylcadaverine (MDC), or 5 μM cytochalasin B (CyB) for 30 min, then treated with hexapodna (2 μg/mL) and incubated at 37 °C for 8 h. The amounts of DNA associated with the cells were measured by flow cytometry. Results are expressed as the % of control (the none group; MFI, 176.2) ± SD of four wells. Data are representative of two independent experiments. *$P < 0.05$ compared with the none (control) group.

IFN-α release from human PBMCs

Because the optimal CpG motif for human TLR9 is reportedly GTCGTT, which is not identical to the optimal murine sequence of GACGTT,[7] polypodna preparations containing human CpG motifs were designed (Table 2). Figure 6, *A* shows the PAGE analysis of ssDNA, tripodna, tetrapodna, pentapodna, and hexapodna. Every sample migrated as a single band on PAGE, indicating efficient formation of each polypodna preparation. Human PBMCs were incubated with ssDNA or polypodna preparations, and the release of IFN-α was measured. Figure 6, *B* shows the IFN-α level in culture media of human PBMCs after the addition of ssDNA or polypodna preparations. Compared with ssDNA, all polypodna preparations, except tripodna, induced significantly higher amounts of IFN-α, although there were no significant differences among the polypodna preparations.

Inhibition of HCV replication by the conditioned media of PBMCs

An HCV subgenomic replicon system was used to examine whether polypodna-induced cytokine production is effective in inhibiting HCV replication in Huh-7 human hepatoma cells. Figure 6, *C* shows the luciferase activity of LucNeo#2 cells after incubation with or without the addition of the conditioned medium of ssDNA- or hexapodna-treated PBMCs. The conditioned medium of the hexapodna-treated PBMCs reduced luciferase activity more effectively than that of the ssDNA-treated PBMCs.

Discussion

There are many strategies to increase the immunostimulatory activity of CpG DNA, including the use of nuclease-resistant DNA analogues.[9,10] We have reported that building up CpG DNA into branched DNA assemblies, such as polypodna and dendrimer-like DNA, is a novel and effective approach to increasing the immunostimulatory activity of CpG DNA.[12,14,17,25] Using mouse macrophage-like RAW264.7 cells, we reported that highly branched DNA assemblies are more effective than conventional single-stranded CpG DNA in

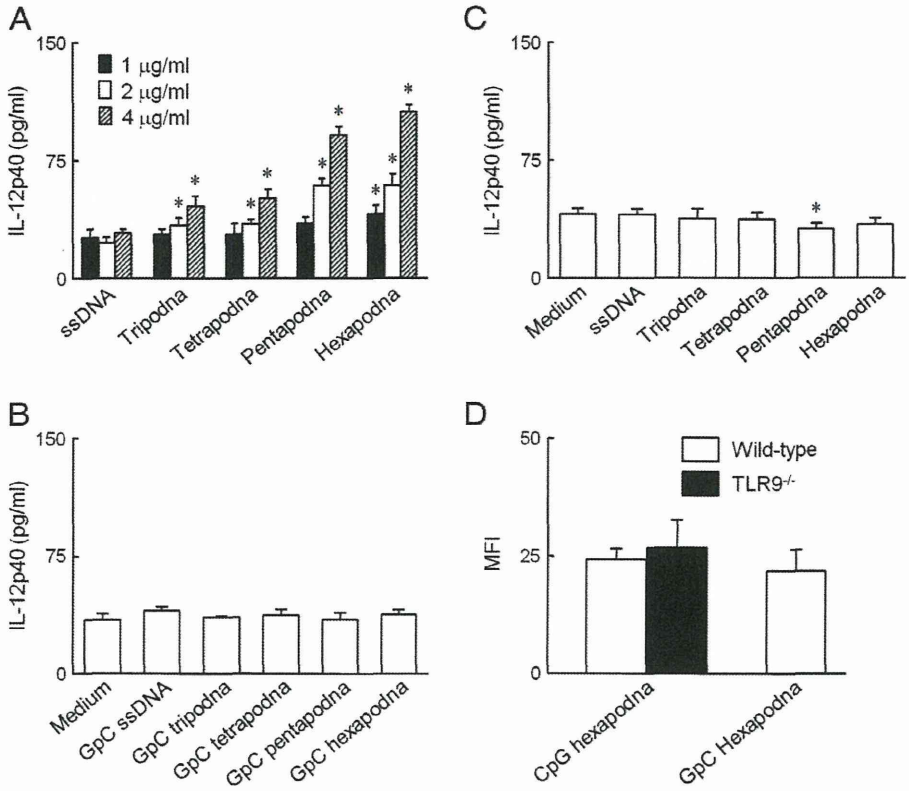

Figure 3. IL-12p40 release and uptake of ssDNA or polypodna after the addition to mouse splenic macrophages. **(A-C)** Splenic macrophages from **(A, B)** wild-type C57/BL6 mice or **(C)** TLR9$^{-/-}$ mice were treated with ssDNA or polypodna containing **(A, C)** CpG or **(B)** GpC motifs at a final concentration of **(A)** 1, 2 or 4 μg/mL or **(B, C)** 2 μg/mL and incubated at 37 °C for 24 h. The concentrations of IL-12p40 in culture media were measured by ELISA. Results are expressed as mean ± SD of four wells. Data are representative of three independent experiments. *$P < 0.05$ compared with **(A)** the ssDNA-treated group or **(B, C)** the medium-treated group. **(D)** Splenic macrophages from wild-type or TLR9$^{-/-}$ mice were treated by Alexa Fluor 488-labelled hexapodna containing CpG or GpC motifs at a final concentration of 2 μg/mL and incubated at 37 °C for 4 h. The amounts of DNA associated with cells were measured by flow cytometry. Results are expressed as mean ± SD of three wells. Data are representative of two independent experiments.

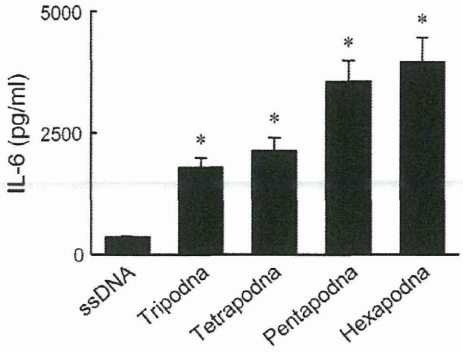

Figure 4. IL-6 release after the addition of ssDNA or polypodna to mouse BMDCs. BMDCs were treated with ssDNA or polypodna at a final concentration of 2 μg/mL and incubated at 37 °C for 24 h. The concentrations of IL-6 in culture media were measured by ELISA. Results are expressed as mean ± SD of three wells. Data are representative of three independent experiments. *$P < 0.05$ compared with the ssDNA-treated group.

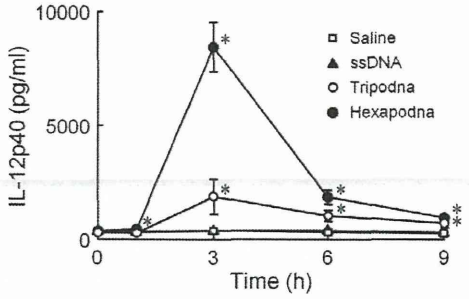

Figure 5. Serum IL-12p40 concentration after intradermal injection of ssDNA or polypodna into mice. Mice received an injection of ssDNA or polypodna at a dose of 100 μg/mouse, and blood was collected from the tail vein at indicated periods of time after injection. The concentrations of IL-12p40 in serum were measured by ELISA. Results are expressed as mean ± SD of six mice. Data are representative of two independent experiments. *$P < 0.05$ compared with the ssDNA-treated group.

inducing cytokine production. We also demonstrated that tetrapodna preparations are more effective than ssDNA in inducing IL-12p40 in mice after injection into the footpad.[25] The present study has extended this finding by showing that other immune cells, i.e., mouse dendritic DC2.4 cells, mouse splenic macrophages, mouse BMDCs, and human PBMCs, respond to CpG polypodna more efficiently than to single-stranded CpG DNA. Similar results of pod number-dependent cytokine production were observed in mice. These results strongly suggest that assembly of CpG DNA into polypod-like or dendritic structures is a versatile and useful method by which

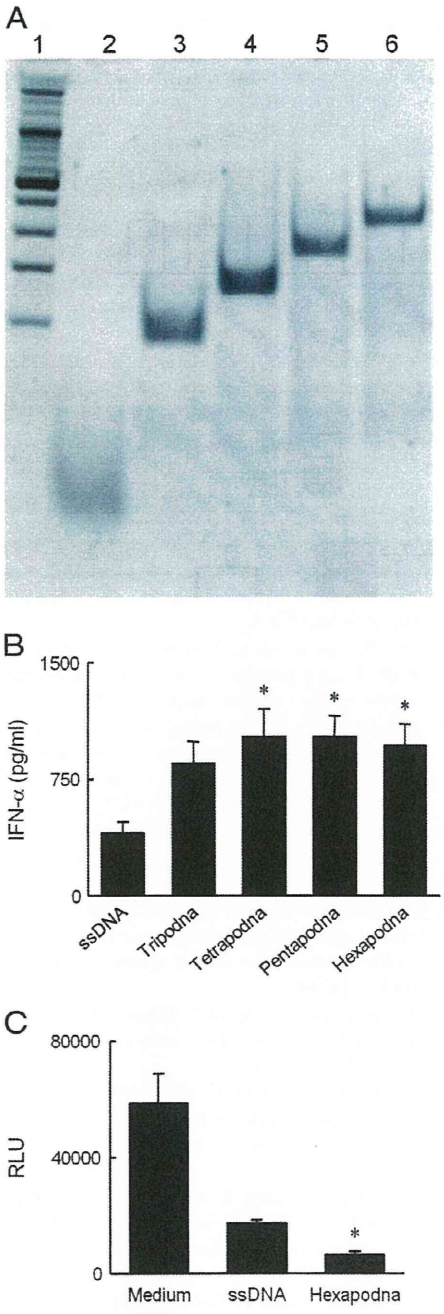

Figure 6. IFN-α release from human PBMCs and inhibition of HCV replication in LucNeo#2 cells after the addition of ssDNA or polypodna to human PBMCs. **(A)** PAGE analysis of polypodna preparations containing human CpG motifs. Each sample was run on a 6% polyacrylamide gel at 200 V for 20 min. Lane 1, 100-bp DNA ladder; lane 2, ssDNA; lane 3, tripodna; lane 4, tetrapodna; lane 5, pentapodna; lane 6, hexapodna. **(B)** PBMCs were treated with ssDNA or polypodna at a final concentration of 2 μg/mL and incubated at 37 °C for 24 h. The concentrations of IFN-α in culture media were measured by ELISA. Results are expressed as mean ± SD of five wells. Data are representative of four independent experiments. *$P < 0.05$ compared with the ssDNA-treated group. **(C)** PBMCs were incubated with ssDNA or polypodna as described above. Then, the conditioned medium was diluted 20-fold, added to LucNeo#2 cells, and the cells were incubated at 37 °C for 24 h. Finally, the luciferase activity of the cell lysates was measured as an indicator of HCV replication. Results are expressed as mean ± SD of five wells. Data are representative of three independent experiments. *$P < 0.05$ compared with the ssDNA-treated group.

to increase the potential of CpG DNA as a vaccine adjuvant without using chemically stabilized DNA analogues.

The detailed mechanism whereby polypodna preparations induce large amounts of cytokines has yet to be fully elucidated, but likely involves the efficient interaction of CpG DNA with its receptor, TLR9. One important factor contributing to the interaction is the cellular uptake of CpG DNA. We found that the cellular uptake of polypodna increased with increasing pod number in RAW264.7 cells[17] and DC2.4 cells (Figure 2, *B*). We also showed that the cellular uptake of hexapodna consisting of 240 nucleotides is higher than that of penta-, tetra- or tripodna of the same number of nucleotides.[17] The significant inhibition of IL-6 production following treatment with the inhibitors (Figure 2, *C*) used suggested that several mechanisms, including endosomal fusion and acidification, clathrin-mediated endocytosis, and phagocytosis, are involved in the uptake of polypodna by the cells. Taken together, these results advocate the hypothesis that DNA assemblies with a bulky structure have a high potential to interact with cells. This hypothesis is supported by experimental evidence that long ODNs are more efficiently taken up by RAW264.7 cells than short ones.[26]

It has been suggested that the cellular uptake of DNA is not mediated by the interaction of TLR9 and CpG DNA.[27] Consistent with this, we found that the cellular uptake of CpG or GpC hexapodna in wild-type or $TLR9^{-/-}$ splenic macrophages was similar (Figure 3, *D*). Our previous study suggests that polypodna shares the uptake mechanism with single- or double-stranded DNA.[17] Studies using phosphorothioate-stabilized CpG DNA concluded that long retention in endosomes explains the high ability of multimeric CpG DNA to produce large amounts of IFN-α from plasmacytoid dendritic cells (pDCs) compared with monomeric CpG DNA.[28,29] Although the detailed mechanism governing the cellular uptake of polypodna remains to be determined, these results suggest that the structure-dependent increase in uptake leads to increased interaction of CpG DNA with TLR9 in endosomes due to its higher concentration and possibly longer retention time in these vesicles.

An important finding of the present study is that the immunostimulatory activity of CpG polypodna is solely dependent on TLR9 ligation. Splenic macrophages and BMDCs of $TLR9^{-/-}$ mice released no significant amount of cytokines when treated with CpG polypodna preparations (Figure 3, *C* and data not shown). When treated with imoquimod, a ligand for TLR7, $TLR9^{-/-}$ splenic macrophages and BMDCs released large amounts of IL-12p40 and IL-6, respectively (data not shown), indicating that the cells have the ability to release cytokines. In addition, these results strongly suggest that TLR9, rather than other intracellular DNA sensors that recognize DNA irrespective of CpG motifs,[24,30–32] is the major polypodna sensor. This was also supported by the almost complete inhibition of CpG hexapodna-induced IL-6 release from DC2.4 cells by chloroquine, an inhibitor of CpG-triggered cytokine release.[33]

Our previous in vivo study indicated that tetrapodna preparations are more effective in inducing IL-12p40 than ssDNA. The present study further confirmed this finding and clearly demonstrated that cytokine production is dependent on the pod number, as observed in experiments using cultured cells. These results provide experimental evidence that polypodna

preparations with many pods are useful for in vivo applications compared with ones with fewer pods.

Human PBMCs consist of several types of cells, including TLR9-positive pDCs. It has been reported that pDCs release IFN-α upon recognition of CpG DNA by TLR9.[8,34] IFN-α activates many types of immune cells, including natural killer cells,[35] DCs,[36] T cells,[37] and B cells,[38] so that the induction of IFN-α release would be useful for the initiation of an immune response. We found that polypodna induced significantly greater amounts of IFN-α secretion from human PBMCs than ssDNA (Figure 6, *B*), although the pod number-dependent increase in human cells was less clear than in the murine counterparts. This might be explained by differences in experimental conditions, including the type of cells and cytokines measured. The PBMCs used would contain only 0.2%-0.8% pDC and many more monocytes and T cells, according to the literature.[34,39] With the exception of pDCs, human monocytes very weakly express TLR9.[7,40] Therefore, cells other than pDCs, such as monocytes, might be involved in IFN-α release from human PBMCs.

The current standard therapy for HCV is a combination of pegylated IFN-α and ribavirin.[41] Our preliminary study using the HCV subgenomic replicon system demonstrated that IFN-α treatment reduced the luciferase activity of the cells, but relatively high IFN-α concentrations (10 IU/mL, corresponding to about 2500 pg/mL, or greater) were required for significant reduction in activity. Because the conditioned medium of human PBMCs containing about 50 pg/mL IFN-α (20-fold diluted) inhibited the luciferase activity to less than 10% (Figure 6, *C*), this clearly suggests that cytokines other than IFN-α are released from human PBMCs by addition of CpG hexapodna. Thus, hexapodna or other highly branched DNA assemblies, including dendrimer-like DNA, containing immunostimulatory sequences, such as CpG motifs, can be effective in inhibiting HCV replication.

In conclusion, we have demonstrated that building CpG DNA into polypod-like structures is a versatile and useful method by which to increase its uptake and cytokine production in many immune cell types, including human PBMCs, and in mice. Based on these findings, we propose that polypodna preparations are natural, biodegradable and highly potent vaccine adjuvants for the treatment of cancer and infectious diseases.

References

1. Manicassamy S, Pulendran B. Modulation of adaptive immunity with Toll-like receptors. *Semin Immunol* 2009;**21**:185-93.
2. Hemmi H, Takeuchi O, Kawai T, Kaisho T, Sato S, Sanjo H, et al. A Toll-like receptor recognizes bacterial DNA. *Nature* 2000;**408**:740-5.
3. Wagner H. Toll meets bacterial CpG-DNA. *Immunity* 2001;**14**:499-502.
4. Pisetsky DS. The origin and properties of extracellular DNA: from PAMP to DAMP. *Clin Immunol* 2012;**144**:32-40.
5. Klinman DM, Yi AK, Beaucage SL, Conover J, Krieg AM. CpG motifs present in bacteria DNA rapidly induce lymphocytes to secrete interleukin 6, interleukin 12, and interferon γ. *Proc Natl Acad Sci U S A* 1996;**93**:2879-83.
6. Sparwasser T, Miethke T, Lipford G, Erdmann A, Häcker H, Heeg K, et al. Macrophages sense pathogens via DNA motifs: induction of tumor necrosis factor-α-mediated shock. *Eur J Immunol* 1997;**27**:1671-9.
7. Bauer S, Kirschning CJ, Häcker H, Redecke V, Hausmann S, Akira S, et al. Human TLR9 confers responsiveness to bacterial DNA via species-specific CpG motif recognition. *Proc Natl Acad Sci U S A* 2001;**98**:9237-42.
8. Krug A, Rothenfusser S, Hornung V, Jahrsdörfer B, Blackwell S, Ballas ZK, et al. Identification of CpG oligonucleotide sequences with high induction of IFN-α/β in plasmacytoid dendritic cells. *Eur J Immunol* 2001;**31**:2154-63.
9. Klinman DM. Immunotherapeutic uses of CpG oligodeoxynucleotides. *Nat Rev Immunol* 2004;**4**:249-58.
10. Vollmer J, Krieg AM. Immunotherapeutic applications of CpG oligodeoxynucleotide TLR9 agonists. *Adv Drug Deliv Rev* 2009;**61**:195-204.
11. Sarmiento UM, Perez JR, Becker JM, Narayanan R. In vivo toxicological effects of rel A antisense phosphorothioates in CD-1 mice. *Antisense Res Dev* 1994;**4**:99-107.
12. Nishikawa M, Matono M, Rattanakiat S, Matsuoka N, Takakura Y. Enhanced immunostimulatory activity of oligodeoxynucleotides by Y-shape formation. *Immunology* 2008;**124**:247-55.
13. Nishikawa M, Mizuno Y, Mohri K, Matsuoka N, Rattanakiat S, Takahashi Y, et al. Biodegradable CpG DNA hydrogels for sustained delivery of doxorubicin and immunostimulatory signals in tumor-bearing mice. *Biomaterials* 2011;**32**:488-94.
14. Rattanakiat S, Nishikawa M, Funabashi H, Luo D, Takakura Y. The assembly of a short linear natural cytosine–phosphate–guanine DNA into dendritic structures and its effect on immunostimulatory activity. *Biomaterials* 2009;**30**:5701-6.
15. Li J, Pei H, Zhu B, Liang L, Wei M, He Y, et al. Self-assembled multivalent DNA nanostructures for noninvasive intracellular delivery of immunostimulatory CpG oligonucleotides. *ACS Nano* 2011;**5**:8783-9.
16. Schüller VJ, Heidegger S, Sandholzer N, Nickels PC, Suhartha NA, Endres S, et al. Cellular immunostimulation by CpG-sequence-coated DNA origami structures. *ACS Nano* 2011;**5**:9696-702.
17. Mohri K, Nishikawa M, Takahashi N, Shiomi T, Matsuoka N, Ogawa K, et al. Design and development of nanosized DNA assemblies in polypod-like structures as efficient vehicles for immunostimulatory CpG motifs to immune cells. *ACS Nano* 2012;**6**:5931-40.
18. Yasuda K, Kawano H, Yamane I, Ogawa Y, Yoshinaga T, Nishikawa M, et al. Restricted cytokine production from mouse peritoneal macrophages in culture in spite of extensive uptake of plasmid DNA. *Immunology* 2004;**111**:282-90.
19. Yoshida H, Nishikawa M, Yasuda S, Mizuno Y, Takakura Y. Cellular activation by plasmid DNA in various macrophages in primary culture. *J Pharm Sci* 2008;**97**:4575-85.
20. O'Mahony DS, Pham U, Iyer R, Hawn TR, Liles WC. Differential constitutive and cytokine-modulated expression of human Toll-like receptors in primary neutrophils, monocytes, and macrophages. *Int J Med Sci* 2008;**5**:1-8.
21. Kadowaki N, Ho S, Antonenko S, Malefyt RW, Kastelein RA, Bazan F, et al. Subsets of human dendritic cell precursors express different toll-like receptors and respond to different microbial antigens. *J Exp Med* 2001;**194**:863-9.
22. Goto K, Watashi K, Murata T, Hishiki T, Hijikata M, Shimotohno K. Evaluation of the anti-hepatitis C virus effects of cyclophilin inhibitors, cyclosporin A, and NIM811. *Biochem Biophys Res Commun* 2006;**343**:879-84.
23. Brasel K, De Smedt T, Smith JL, Maliszewski CR. Generation of murine dendritic cells from flt3-ligand-supplemented bone marrow cultures. *Blood* 2000;**96**:3029-39.
24. Takaoka A, Wang Z, Choi MK, Yanai H, Negishi H, Ban T, et al. DAI (DLM-1/ZBP1) is a cytosolic DNA sensor and an activator of innate immune response. *Nature* 2007;**448**:501-5.
25. Mohri K, Takahashi N, Nishikawa M, Kusuki E, Shiomi T, Takahashi Y, et al. Increased immunostimulatory activity of polypod-like structured DNA by ligation of the terminal loop structures. *J Control Release* 2012;**163**:285-92.
26. Roberts TL, Dunn JA, Terry TD, Jennings MP, Hume DA, Sweet MJ, et al. Differences in macrophage activation by bacterial DNA and CpG-containing oligonucleotides. *J Immunol* 2005;**175**:3569-76.

27. Trombone AP, Silva CL, Lima KM, Oliver C, Jamur MC, Prescott AR, et al. Endocytosis of DNA-Hsp65 alters the pH of the late endosome/lysosome and interferes with antigen presentation. *PLoS One* 2007;**2**:e923.
28. Honda K, Ohba Y, Yanai H, Negishi H, Mizutani T, Takaoka A, et al. Spatiotemporal regulation of MyD88-IRF-7 signalling for robust type-I interferon induction. *Nature* 2005;**434**:1035-40.
29. Guiducci C, Ott G, Chan JH, Damon E, Calacsan C, Matray T, et al. Properties regulating the nature of the plasmacytoid dendritic cell response to Toll-like receptor 9 activation. *J Exp Med* 2006;**203**:1999-2008.
30. Hornung V, Ablasser A, Charrel-Dennis M, Bauernfeind F, Horvath G, Caffrey DR, et al. AIM2 recognizes cytosolic dsDNA and forms a caspase-1-activating inflammasome with ASC. *Nature* 2009;**458**:514-8.
31. Unterholzner L, Keating SE, Baran M, Horan KA, Jensen SB, Sharma S, et al. IFI16 is an innate immune sensor for intracellular DNA. *Nat Immunol* 2010;**11**:997-1004.
32. Sun L, Wu J, Du F, Chen X, Chen ZJ. Cyclic GMP-AMP synthase is a cytosolic DNA sensor that activates the type I interferon pathway. *Science* 2013;**339**:786-91.
33. Rutz M, Metzger J, Gellert T, Luppa P, Lipford GB, Wagner H, et al. Toll-like receptor 9 binds single-stranded CpG-DNA in a sequence- and pH-dependent manner. *Eur J Immunol* 2004;**34**:2541-50.
34. Liu YJ. IPC: professional type 1 interferon-producing cells and plasmacytoid dendritic cell precursors. *Annu Rev Immunol* 2005;**23**: 275-306.
35. Trinchieri G, Santoli D. Anti-viral activity induced by culturing lymphocytes with tumor-derived or virus-transformed cells. Enhancement of human natural killer cell activity by interferon and antagonistic inhibition of susceptibility of target cells to lysis. *J Exp Med* 1978;**147**: 1314-33.
36. Montoya M, Schiavoni G, Mattei F, Gresser I, Belardelli F, Borrow P, et al. Type I interferons produced by dendritic cells promote their phenotypic and functional activation. *Blood* 2002;**99**:3263-71.
37. Le Bon A, Durand V, Kamphuis E, Thompson C, Bulfone-Paus S, Rossmann C, et al. Direct stimulation of T cells by type I IFN enhances the $CD8^+$ T cell response during cross-priming. *J Immunol* 2006;**176**:4682-9.
38. Le Bon A, Thompson C, Kamphuis E, Durand V, Rossmann C, Kalinke U, et al. Cutting edge: enhancement of antibody responses through direct stimulation of B and T cells by type I IFN. *J Immunol* 2006;**176**:2074-8.
39. Baechler EC, Batliwalla FM, Karypis G, Gaffney PM, Ortmann WA, Espe KJ, et al. Interferon-inducible gene expression signature in peripheral blood cells of patients with severe lupus. *Proc Natl Acad Sci U S A* 2003;**100**:2610-5.
40. Hornung V, Rothenfusser S, Britsch S, Krug A, Jahrsdörfer B, Giese T, et al. Quantitative expression of toll-like receptor 1-10 mRNA in cellular subsets of human peripheral blood mononuclear cells and sensitivity to CpG oligodeoxynucleotides. *J Immunol* 2002;**168**:4531-7.
41. Fried MW, Shiffman ML, Reddy KR, Smith C, Marinos G, Gonçales Jr FL, et al. Peginterferon alfa-2a plus ribavirin for chronic hepatitis C virus infection. *N Engl J Med* 2002;**347**:975-82.

molecular pharmaceutics

Article

pubs.acs.org/molecularpharmaceutics

Expression Profile-Dependent Improvement of Insulin Sensitivity by Gene Delivery of Interleukin-6 in a Mouse Model of Type II Diabetes

Hanae Mukumoto, Yuki Takahashi, Mitsuru Ando, Makiya Nishikawa, and Yoshinobu Takakura*

Department of Biopharmaceutics and Drug Metabolism, Graduate School of Pharmaceutical Sciences, Kyoto University, Sakyo-ku, Kyoto 606-8501, Japan

ABSTRACT: Type II diabetes is one of the most problematic metabolic disorders and is associated with secondary conditions such as heart disease and eye complications. Interleukin-6 (IL-6), a multifunctional cytokine, could influence conditions of altered glucose metabolism such as insulin resistance in diabetic patients. However, a consensus about the role of IL-6 on glucose metabolism has not been reached. The aim of the present study is to investigate whether the expression of IL-6 affects glucose metabolism in diet-induced obesity (DIO) mice, a model of type II diabetes and obesity, using gene delivery of IL-6. DIO mice received hydrodynamic or intramuscular injection of IL-6-expressing plasmid to investigate the importance of the site of IL-6 expression. DIO mice that received a sustained IL-6 gene transfer showed similar glucose levels to lean mice in a glucose tolerance test. DIO mice exhibited reduced food intake and low body and epididymal fat weights after IL-6 gene transfer. IL-6 gene delivery reduced the mRNA expression of metabolism-related genes in the liver, skeletal muscle, and adipose tissue of DIO mice. The metabolic status of DIO mice receiving intramuscular injections was moderately better than that of DIO mice receiving hydrodynamic injections. The infiltration of inflammatory cells into the sites where the IL-6-expressing plasmid DNA was delivered was observed. Transient expression of IL-6 had limited effects on all parameters examined. These results indicate that the expression of IL-6 has an effect on obesity and the metabolism of glucose and lipid in diabetic mice and that the expression site of IL-6 is not an important factor.

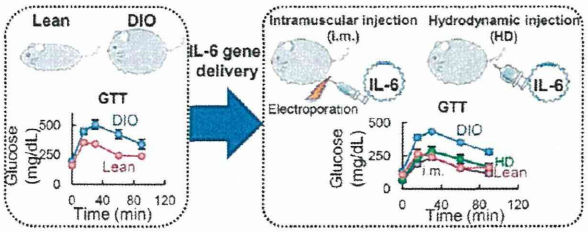

KEYWORDS: *IL-6, insulin resistance, plasmid DNA, skeletal muscle, liver*

INTRODUCTION

Type II diabetes is one of the most problematic metabolic disorders because of its associated conditions, such as heart diseases and eye complications. Physical exercise and diet therapy are the first choices to treat type II diabetes patients.[1] However, the progression of the disease results in an increase in the number of patients who have to take oral medications. Even at this stage, exercise therapy is effective in increasing the therapeutic effect of oral medications such as acarbose, rosiglitazone, and losartan.[1−3] In addition to increasing energy expenditure, which is effective in losing weight, physical exercise also produces various changes in the body. Recently, it has been found that the concentrations of several cytokines in the serum increase during physical exercise.[4,5]

Of the cytokines that are reported to increase during exercise, interleukin (IL)-6 is produced in working muscles, which results in an increase in the blood concentration of IL-6 up to 100-fold.[6] Considering the fact that exercise improves glucose metabolism, such as insulin sensitivity, and that IL-6 is a typical cytokine induced by exercise, a close relationship between IL-6 and glucose metabolism has been suggested.[7−10] The beneficial effects of IL-6 in diabetes, such as an increase in insulin sensitivity, improvement in the obese state, and an increase in central leptin action, have been demonstrated by several studies.[11−14] However, Klover et al. reported that chronic exposure to IL-6 reduced insulin sensitivity in the liver.[15] Because previous in vitro studies reported that IL-6 increased the insulin sensitivity of muscle cells but reduced the sensitivity of hepatocytes,[16−21] cell-type-specific responses to IL-6 may be a reason for the controversy regarding the effect of IL-6 on insulin sensitivity. In addition, the different periods of IL-6 exposure (i.e., the different IL-6 pharmacokinetic profiles between the different studies) may also account for the controversy. However, the relationship between the time profile of IL-6 exposure and its effect on glucose metabolism has not been investigated in detail in whole animal models.

In the present study, we investigated the relationship between the expression profile of IL-6 and the effect of IL-6 in DIO mice. To obtain different pharmacokinetics of IL-6, we used two types of IL-6-expressing plasmid vectors, each of which shows transient or sustained transgene expression. The effects of IL-6 gene transfer on glucose and lipid homeostasis in the whole body as well as the metabolic status in skeletal muscle, liver, and adipose tissue were investigated to evaluate the pharmacodynamics of IL-6. In addition, to investigate

Received: May 17, 2013
Revised: August 22, 2013
Accepted: September 11, 2013
Published: September 24, 2013

whether the production site of IL-6 is important for its effect on insulin sensitivity, the IL-6 transgene was delivered to the liver or skeletal muscle.

EXPERIMENTAL SECTION

Animals. Four-week-old male C57BL/6J mice were purchased from Japan SLC, Inc. (Shizuoka, Japan). Mice were fed a high-fat diet (D12492-RodentDiet with 60 kcal % fat, Research Diets, New Brunswick, Canada) or a normal diet (D12450B-RodentDiet with 10 kcal % fat, Research Diets) for 12 weeks to obtain DIO and lean mice, respectively. All protocols for the animal experiments were approved by the Animal Experimentation Committee of the Graduate School of Pharmaceutical Science of Kyoto University.

Plasmid DNA Construction. mRNA was extracted from RAW264.7 cells using Sepasol RNA I super (Nacalai Tesque, Kyoto, Japan), and a cDNA sample was prepared using SuperScript II (Invitrogen, Carsbad, CA, USA). An IL-6 cDNA fragment was amplified from the RAW264.7 cDNA sample and subcloned into the EcoR V/Xba I sites of the pcDNA 3.1 vector (Invitrogen) to construct pCMV-IL-6. pCpG-IL-6 was constructed by inserting the murine IL-6 cDNA fragment from pCMV-IL-6 into the Nhe I/Nco I sites of the pCpG-mcs vector (Invivogen, San Diego, CA, USA). pcDNA3.1 and pCpG-mcs, which encode no cDNA, were used as mock vectors for pCMV-IL-6 and pCpG-IL-6, respectively.

Plasmid DNA Administration. Mice received an intramuscular or hydrodynamic injection of naked plasmid DNA (pDNA) for the delivery of the pDNA to the skeletal muscle or liver, respectively. For intramuscular gene transfer, mice received an intramuscular injection of 10 units of hyaluronidase (Sigma-Aldrich, St. Louis, MO, USA) into the gastrocnemius muscle of both hindlegs 2 h before pDNA administration to increase the delivery efficiency of pDNA.[22] Next, the indicated dose of pDNA dissolved in saline was injected into the muscle of both hindlegs. Immediately after the injection, electroporation was applied to each injection site (175 V/cm, 20 ms, 2 Hz, 10 pulses) using a pair of 1 cm^2 forceps-type electrodes connected to a rectangular direct-current generator (CUY-21, Nepagene, Chiba, Japan). Because our preliminary study showed that the intramuscular delivery of the pCMV vector could obtain a higher level of transgene expression than that of the pCpG vector and that the duration of transgene expression was comparable between these two vectors, the pCMV vector was used for the intramuscular gene delivery. For the hepatic gene transfer, the indicated dose of pDNA was dissolved in saline and injected into the tail vein of mice over a period of 5 s.[23] To obtain a transient or continuous transgene expression profile after hepatic gene transfer, the pCMV vector or pCpG vector was utilized, respectively.[24,25]

Measurement of the Serum Concentrations of IL-6, Insulin, Nonesterified Fatty Acids (NEFA), Triglyceride (TG), Cholesterol, and Amyloid A. Blood samples were obtained from the tail vein of mice at the indicated times after gene transfer, kept at 4 °C for 2 h to allow clotting, and centrifuged at 8000*g* for 20 min to obtain serum. The concentration of IL-6 in the serum was measured by an enzyme-linked immunosorbent assay (ELISA) using OptEIA sets (BD Biosciences, San Diego, CA, USA). The concentration of insulin was measured using an ELISA kit (Mercodia, Uppsala, Sweden). The concentration of NEFA, TG, and cholesterol was measured using a kit (Wako Pure Chemical Industries, Osaka, Japan). The concentration of serum amyloid A (SAA) was measured using an SAA Mouse ELISA Kit (Invitrogen).

mRNA Quantification. Total RNA was extracted from approximately 100 mg tissue samples using Sepasol RNA I Super (Nakalai Tesque). After the removal of contaminating DNA by DNase I (Takara Bio, Shiga, Japan), reverse transcription was performed using a ReverTra Ace qPCR RT kit (TOYOBO, Osaka, Japan) followed by ribonuclease H treatment (Takara Bio). For a quantitative analysis of mRNA expression, real-time polymerase chain reaction (PCR) was carried out with total cDNA using the Kapa SYBR FAST ABI Prism 2× qPCR Master Mix (Kapa Biosystems, Boston, MA, USA). The oligonucleotide primers used for amplification were IL-6 (forward) 5′-GTTCTCTGGGAAATCGTGGA-3′ and (reverse) 5′-TGTACTCCAGGTAGCTATGG-3′; suppressors of cytokine signaling 3 (SOCS-3) (forward) 5′-AAGGGAGGCAGATCAACAGA-3′ and (reverse) 5′-TGGGACAGAGGGCATTTAAG-3′; pyruvate kinase 1 (PK-1) (forward) 5′-AAGACAGTGTGGGTGGACTACCA-3′ and (reverse) 5′-CGTCAATGTAGATGCGGCC-3′; pyruvate kinase 3 (PK-3) (forward) 5′-GCCGCCTGGACATTGACTC-3′ and (reverse) 5′-CATGAGAGAAATTCAGCCGAG-3′; glucose-6-phosphatase (G6Pase) (forward) 5′-TCGGAGACTGGTTCAACCTC-3′ and (reverse) 5′-AGGTGACAGGGAACTGCTTTAT-3′; phosphoenolpyruvate carboxykinase (PEPCK) (forward) 5′-GGTGTTTACTGGGAAGGCATC-3′ and (reverse) 5′-CAATAATGGGGCACTGGCTG-3′; glycogen synthase 1 (GYS-1) (forward) 5′-GAACGCAGTGCTTTTCGAGG-3′ and (reverse) 5′-CCAGATAGTAGTTGTCACCCCAT-3′; glycogen synthase 2 (GYS-2) (forward) 5′-ACCAAGGCCAAAACGACAG-3′ and (reverse) 5′-GGGCTCACATTGTTCTACTTGA-3′; long chain acyl-CoA dehydrogenase (LCAD) (forward) 5′-TCTTTTCCTCGGAGCATGACA-3′ and (reverse) 5′-GACCTCTCTACTCACTTCTCCAG-3′; peroxisome proliferator-activated receptor α (PPAR-α) (forward) 5′-TGTCGAATATGTGGGGACAA-3′ and (reverse) 5′-AATCTTGCAGCTCCGATCAC-3′; peroxisome proliferator-activated receptor γ (PPAR-γ) (forward) 5′-CCCACCAACTTCGGAATCA-3′ and (reverse) 5′-TGCGAGTGGTCTTCCATCAC-3′; acetyl-CoA carboxylase 1 (ACC-1) (forward) 5′-GCCTCTTCCTGACAAACGAG-3′ and (reverse) 5′-TGACTGCCGAAACATCTCTG-3′; sterol regulatory element-binding protein 1c (SREBP-1c) (forward) 5′-CCCTGTGTGTACTGGCCTTT-3′ and (reverse) 5′-TTGCGATGTCTCCAGAAGTG-3′; uncoupling protein 2 (UCP-2) (forward) 5′-GCCTCTGGAAAGGGACTTCTC-3′ and (reverse) 5′-ACCAGCTCAGCACAGTTGACA-3′; and cyclophilin (forward) 5′-GGAGATGGCACAGGAGGAA-3′ and (reverse) 5′-GCCCGTAGTGCTTCAGCTT-3′. Amplified products were detected via the intercalation of the fluorescent dye using a StepOnePlus Real Time PCR System (Applied Biosystems, Foster City, CA, USA). The mRNA expression of target genes was normalized against the mRNA level of cyclophilin.

Glucose Tolerance Test. At the indicated time points after IL-6 gene transfer, glucose tolerance tests (GTTs) were performed. In brief, mice received an intraperitoneal injection of glucose (1 g/kg body weight) after a 12 h period of starvation. The glucose concentration in the blood was then measured using an automatic glucose analyzer (Accucheck, Roche Diagnostics, Indianapolis, IN, USA).

Histological Analysis. Mice were killed on day 14 after gene transfer, and the gastrocnemius muscle, liver, and epididymal fat samples were collected, fixed in 4% paraformal-

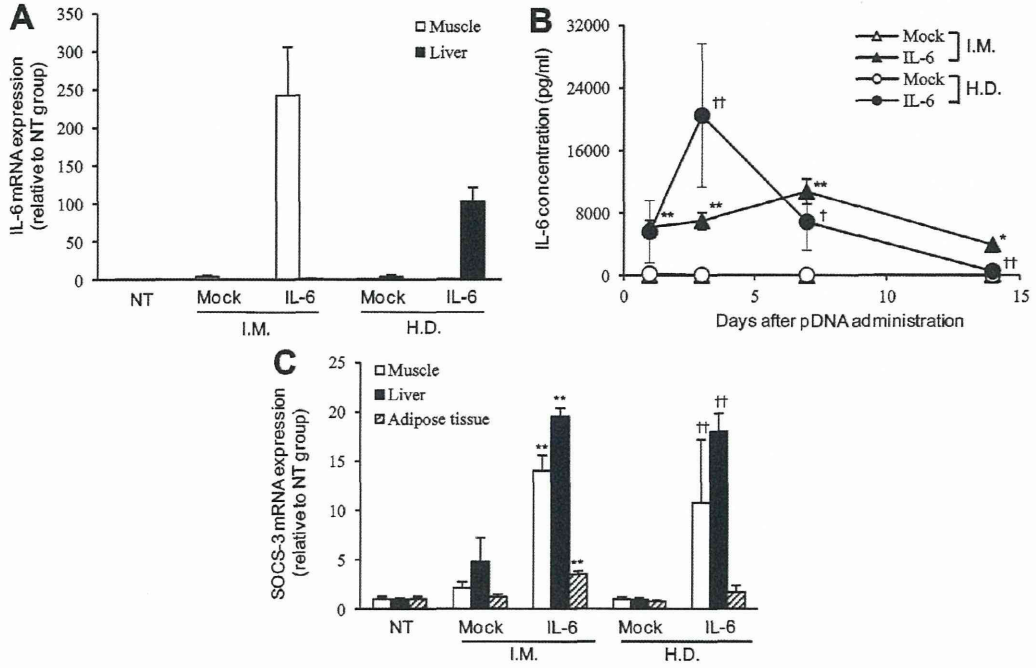

Figure 1. IL-6 and SOCS-3 expression after gene delivery into muscle and liver. DIO mice received an intramuscular injection (I.M.) of pcDNA3.1 (mock) (200 μg/mouse) or pCMV-IL-6 (200 μg/mouse) or a hydrodynamic injection (H.D.) of pCpG-mcs (mock) (0.75 μg/g bodyweight) or pCpG-IL-6 (0.75 μg/g bodyweight). (A) mRNA expression of IL-6 in the muscle and liver on day 14. The results are expressed as the mean + SE of five mice except for the H.D. injection in the pCpG-IL-6 group (n = 3). (B) Time course of the concentration of IL-6 in the serum after gene delivery. The results are expressed as the mean ± SE of five mice except for the H.D. injection in the pCpG-IL-6 group (n = 3). (C) mRNA expression of SOCS-3, an IL-6-induced gene, in the muscle, liver, and adipose tissue on day 14. The results are expressed as the mean + SE of five mice except for the H.D. injection in the pCpG-IL-6 group (n = 3). $^{**}P < 0.01$ compared with the mock intramuscular injection group and $^{\dagger}P < 0.05$ and $^{\dagger\dagger}P < 0.01$ compared with the mock hydrodynamic injection group.

dehyde, embedded in paraffin, sectioned, and stained with hematoxylin and eosin (HE). The stained samples were viewed under a microscope (Biozero BZ-8000, KEYENCE) for histological evaluation.

Statistical Analysis. Differences were statistically evaluated by student's t test. A P value of less than 0.05 was considered to be statistically significant. The area under the serum concentration–time curve (AUC) and the mean retention time (MRT) were calculated using a moment analysis method.[26] These parameters were calculated for each animal.

RESULTS

IL-6 Expression and IL-6-Induced SOCS-3 Expression in DIO Mice after IL-6 Gene Delivery. To obtain sustained IL-6 expression in the skeletal muscle (gastrocnemius muscle) and in the liver, mice received an intramuscular injection of pCMV-IL-6 or a hydrodynamic injection of pCpG-IL-6, respectively. IL-6 mRNA expression was increased in the skeletal muscle or liver of mice that received an intramuscular or a hydrodynamic injection of IL-6-expressing pDNA, respectively (Figure 1A). IL-6 mRNA expression in the liver was hardly increased in the mice that received an intramuscular injection of IL-6-expressing pDNA. On the contrary, the mRNA expression in the muscle was hardly increased in the mice that received a hydrodynamic injection of IL-6 expressing pDNA. These mice showed a sustained level of IL-6 in the serum for at least 2 weeks after gene delivery (Figure 1B). The AUC values of the IL-6 concentration in the serum were 100 ± 20 and 83 ± 15 ng/(mL·day) in mice that received an intramuscular or a hydrodynamic injection of IL-6-expressing pDNA, respectively. The MRT values were 6.3 ± 0.4 and 3.8 ± 0.6 days for the intramuscular or hydrodynamic group, respectively. As an indicator of the local concentration of IL-6 in the skeletal muscle, liver, and epididymal adipose tissue, we measured the mRNA expression of SOCS-3 in these tissues because SOCS-3 is a typical IL-6-induced gene. IL-6 gene delivery significantly increased the SOCS-3 mRNA expression in skeletal muscle and liver to a similar extent in both cases (Figure 1C). However, the SOCS-3 mRNA expression in adipose tissue was greatly increased after intramuscular injection of IL-6-expressing pDNA, whereas it was slightly, but not significantly, increased after hydrodynamic injection of IL-6-expressing pDNA.

Effect of IL-6 Gene Delivery on GTTs and Serum Insulin Concentration. GTTs were performed on days 7 and 13 after gene transfer (Figure 2). After an intraperitoneal injection of glucose, the untreated and mock-treated DIO mice showed higher glucose levels over the time periods studied than the lean mice. In contrast, the DIO mice that received a hydrodynamic and intramuscular injection of IL-6-expressing pDNA showed similar glucose levels to those of the lean mice, which implies the improvement of insulin sensitivity by IL-6 gene delivery. The serum concentration of insulin in the untreated DIO mice and mock-treated DIO mice was higher than that in the lean mice. IL-6 gene delivery reduced the serum insulin concentration in DIO mice, which suggests the improvement in their metabolic status by IL-6 gene delivery.

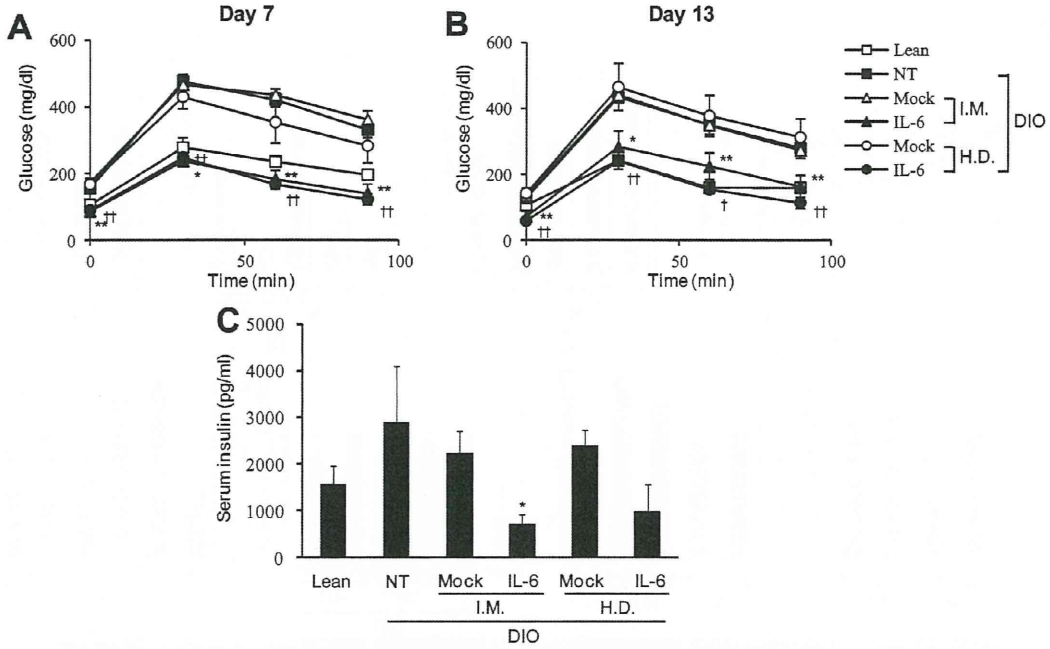

Figure 2. Effect of IL-6 gene delivery into the muscle and liver on the glucose tolerance test. DIO mice received an intramuscular injection (I.M.) of pcDNA3.1 (mock) (200 μg/mouse) or pCMV-IL-6 (200 μg/mouse) or a hydrodynamic injection (H.D.) of pCpG-mcs (mock) (0.75 μg/g bodyweight) or pCpG-IL-6 (0.75 μg/g bodyweight). (A, B) On (A) day 7 and (B) day 13, glucose tolerance tests were performed. After a 12 h fast, the mice received an intraperitoneal injection of glucose (1 g/kg), and the glucose concentration was determined in tail blood samples. The results are expressed as the mean ± SE of five mice except for the H.D. injection in the pCpG-IL-6 group ($n = 3$). (C) On day 14, the serum concentration of insulin was measured by ELISA. The results are expressed as the mean + SE of five mice except for the I.M. injection of pCMV-IL-6 group ($n = 4$) and the H.D. injection in the pCpG-IL-6 group ($n = 3$). $^{*}P < 0.05$ and $^{**}P < 0.01$ compared with the mock intramuscular injection group. $^{\dagger}P < 0.05$ and $^{\dagger\dagger}P < 0.01$ compared with the mock hydrodynamic injection group.

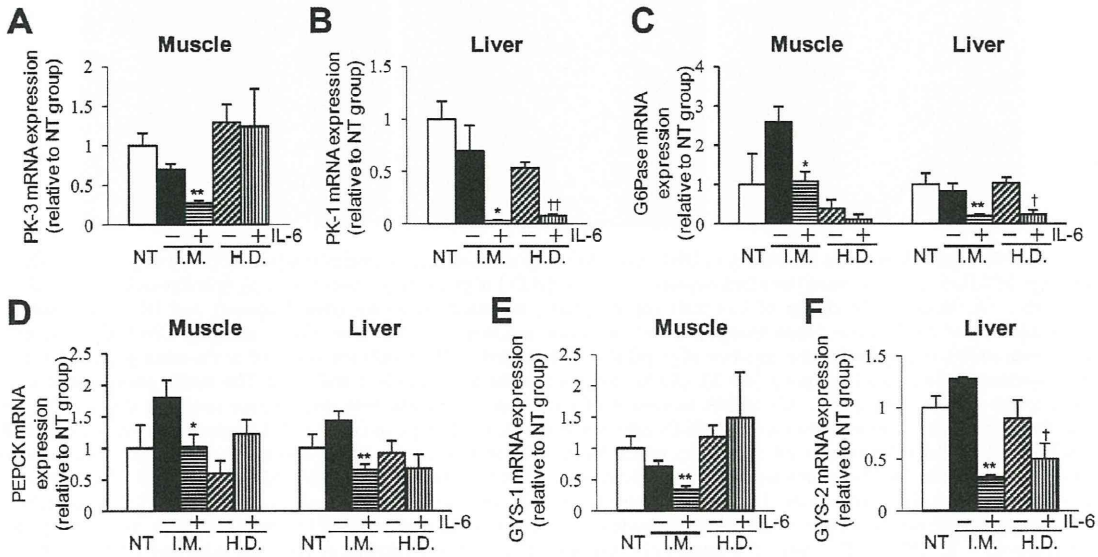

Figure 3. Effect of IL-6 gene delivery on the mRNA expression of glucose metabolism-related genes in the muscle and liver. DIO mice received an intramuscular injection (I.M.) of pcDNA3.1 (mock) (200 μg/mouse) or pCMV-IL-6 (200 μg/mouse) or a hydrodynamic injection (H.D.) of pCpG-mcs (mock) (0.75 μg/g bodyweight) or pGpG-IL-6 (0.75 μg/g bodyweight). (A, B) mRNA expression of (A) PK-3 and (B) PK-1 in the muscle and liver on day 14, respectively. (C, D) mRNA expression of (C) G6Pase and (D) PEPCK in the muscle and liver on day 14. (E, F) mRNA expression of (E) GYS-1 in the muscle and (F) GYS-2 in the liver on day 14. The results are expressed as the mean + SE of five mice except for the H.D. injection in the pCpG-IL-6 group ($n = 3$). $^{*}P < 0.05$ and $^{**}P < 0.01$ compared with the mock intramuscular injection group. $^{\dagger}P < 0.05$ and $^{\dagger\dagger}P < 0.01$ compared with the mock hydrodynamic injection group.

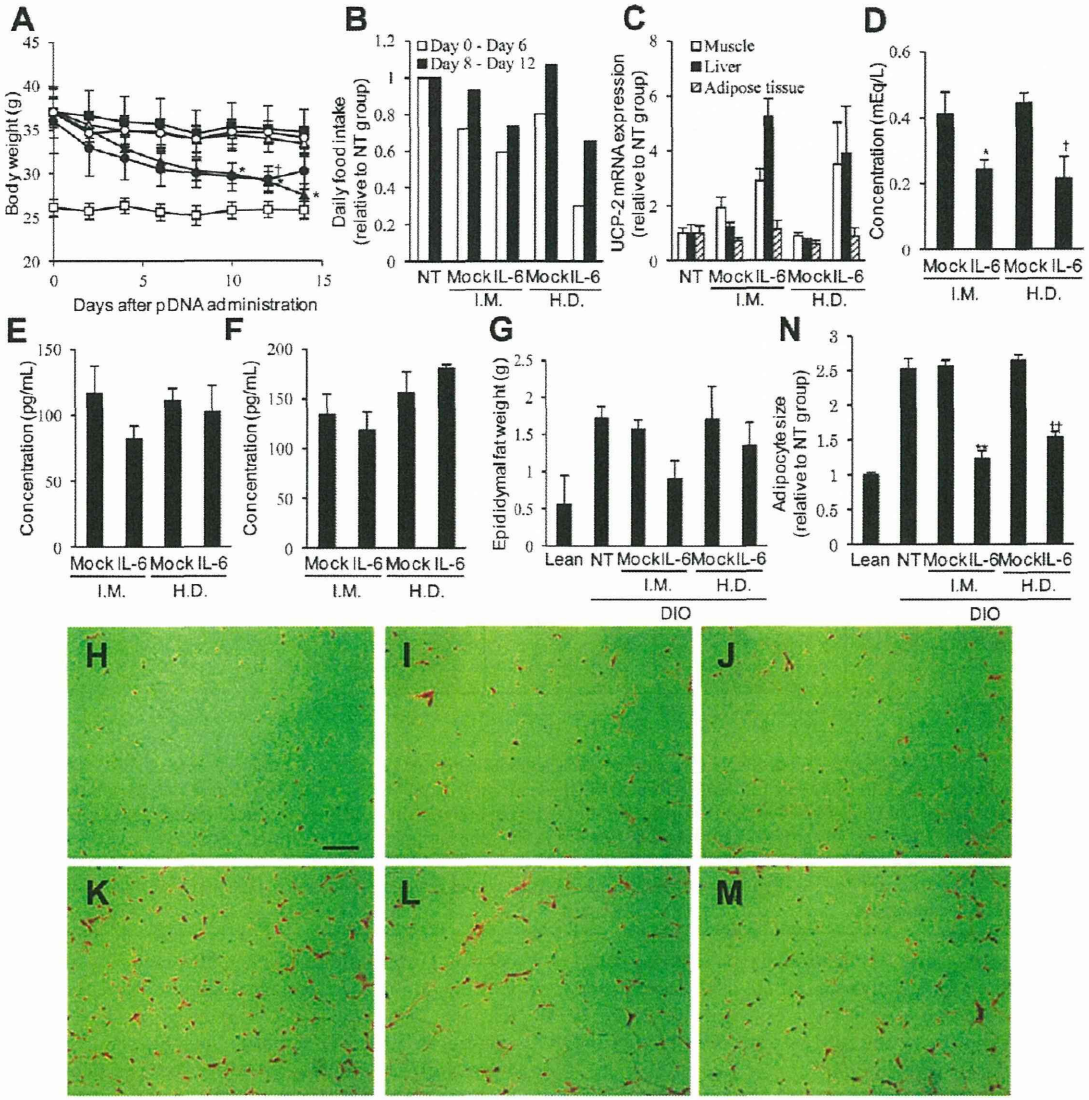

Figure 4. Effect of IL-6 gene delivery on the obesity of DIO mice. DIO mice received an intramuscular injection (I.M.) of pcDNA3.1 (mock) (200 μg/mouse) or pCMV-IL-6 (200 μg/mouse) or a hydrodynamic injection (H.D.) of pCpG-mcs (mock) (0.75 μg/g bodyweight) or pGpG-IL-6 (0.75 μg/g bodyweight). (A) Body weight change of lean mice (open square), untreated DIO mice (closed square), and DIO mice treated with an intramuscular injection of mock vector (open triangle), an intramuscular injection of pCMV-IL-6 (closed triangle), a hydrodynamic injection of mock vector (open circle), or a hydrodynamic injection of pCpG-IL-6 (closed circle). The results are expressed as the mean ± SE of five mice except for the H.D. injection in the pCpG-IL-6 group (n = 3). (B) Relative food intake from days 0–6 and 8–12. The results are expressed as the mean relative value to the no-treatment group. (C) mRNA expression of UCP-2 in the muscle, liver, and adipose tissue on day 14. The results are expressed as the mean + SE of five mice except for the H.D. injection in the pCpG-IL-6 group (n = 3). (D) Serum concentration of NEFA on day 14. The results are expressed as the mean + SE of five mice except for the H.D. injection in the pCpG-IL-6 group (n = 3). (E) Serum concentration of TG and cholesterol on day 14. The results are expressed as the mean + SE of four mice except for the H.D injection in the mock groups (n = 5). (F) Serum concentration of cholesterol on day 14. The results are expressed as the mean + SE of four mice except for the H.D injection in the mock groups (n = 5). (G) Epididymal fat weight on day 14. The results are expressed as the mean + SE of five mice except for the H.D. injection in the pCpG-IL-6 group (n = 3). (H–M) Representative images of HE-stained adipose tissue sections of (H) lean mice and DIO mice that were (I) untreated or (J) treated with an intramuscular injection of mock vector, (K) an intramuscular injection of pCMV-IL-6, (L) a hydrodynamic injection of mock vector, or (M) a hydrodynamic injection of pCpG-IL-6. The scale bar is 100 μm. (N) Relative adipocyte size calculated from the adipocyte numbers per field on day 14. The results are expressed as the mean + SE of five images. *P < 0.05 and **P < 0.01 compared with the mock intramuscular injection group. †P < 0.05 and ††P < 0.01 compared with the mock hydrodynamic injection group.

Effect of IL-6 Gene Delivery on the mRNA Expression of Glucose Metabolism-Related Genes in the Skeletal Muscle and Liver. To investigate whether IL-6 improves glucose metabolism via the regulation of glucose metabolism-related genes at molecular level, we examined their mRNA expression. The mRNA expression level of all of the genes investigated significantly decreased in the skeletal muscle and liver following the intramuscular injection of IL-6-expressing